Deconfinement phase transition in hybrid neutron stars from the Brueckner theory with three-body forces and a quark model with chiral mass scaling

G. X. Peng

China Center of Advanced Science and Technology (World Laboratory), P. O. Box 8730, Beijing 100080, China
Theoretical Physics Center for Science Facilities, Institute of High Energy Physics, CAS, Beijing 100049, China
Department of Physics, Graduate University, Chinese Academy of Sciences, Yuquan Rd. 19A, Beijing 100049, China

A. Li

Dipartimento di Fisica e Astronomia, Universitá di Catania, viale Andrea Doria 6, I-95125 Catania, Italy
Department of Physics and Institute of Theoretical Physics and Astrophysics, Xiamen University, Xiamen 361005, China

U. Lombardo

Laboratori Nazionali del Sud, Istituto Nazionale di Fisica Nucleare, Via S. Sofia 62, I-95123 Catania, Italy
Dipartimento di Fisica e Astronomia, Universitá di Catania, viale Andrea Doria 6, I-95125 Catania, Italy

We study the properties of strange quark matter in equilibrium with normal nuclear matter. Instead of using the conventional bag model in quark sector, we achieve the confinement by a density-dependent quark mass derived from in-medium chiral condensates. In nuclear matter, we adopt the equation of state from the Brueckner-Bethe-Goldstone approach with three-body forces. It is found that the mixed phase can occur, for a reasonable confinement parameter, near the normal nuclear saturation density and goes over to pure quark matter at about 5 times the saturation. The onset of mixed and quark phases is compatible with the observed class of low-mass neutron stars, but it hinders the occurrence of kaon condensation.

I. INTRODUCTION

By far the study of neutron stars (NS) has been mainly focused on the relationship between the equation of state (EOS) of nuclear matter and the observed maximum mass. The connection has been achieved by solving the hydrostatic equilibrium equations based on general relativity. The first-generation observed masses exhibited an average value around 1.5 solar masses. This value requires a soft EOS that can be easily obtained by introducing new degrees of freedom like hyperons, kaons, or quarks accompanied or not by a phase transition. Sometimes the softening was so large that the neutron star is predicted to collapse into a black hole, as for the SN1987A [1]. In the new generation of observations the masses are distributed within a large range, up to two solar masses, that requires a stiff EOS, i.e., hadronic matter without new degrees of freedom. Because it is hard to imagine pure hadronic matter sustaining the high pressure predicted in the inner core, new scenarios have to be advanced to explain the coexistence, in the phenomenology of neutron stars, of low- and high-mass spectra.

Recently [2] it has been argued that the two observed classes of neutron stars might correspond to two different evolutionary scenarios of neutron stars. In one case, the hot and dense remnant of the supernova explosion rapidly evolves into a hybrid star, where the transition to a quark phase softens the nuclear matter so that $M \approx 1.5 M_\odot$; in the other case a slow evolution could lead the neutron star to a large mass via a mass accreting from the coupling with a white dwarf. From this point of view the destiny of the remnant is strongly affected by the initial conditions, i.e., density, temperature, leptonization degree, etc. For instance, if the mass of the remnant is below the mass threshold for quark nucleation the transition to the quark phase is forbidden [3]. If the mass is slowly accreting the transition is allowed. The role of temperature or other parameters defining the initial state of a newborn neutron star has not yet been studied.

To investigate the possible phase transition to quark matter in neutron stars, we need also to know the EOS of quark matter. Although we have in hand the fundamental theory of strong interactions, i.e., quantum chromodynamics (QCD), we still do not know the true ground state. It is now generally expected that quark matter is in the color-flavor locked phase (CFL) [4] at extremely high densities when the finite current mass of strange quarks becomes unimportant. In the density range from nuclear saturation to CFL, there may exist a rich and varied landscape of phases, e.g., the 2SC, g2SC, gCFL, etc. Presently, however, these phases suffer from the so-called chromomagnetic instability problem for both the two- [5] and three-flavor [6–8] cases. However, experiments show that quarks become asymptotically free rather slowly [9]. Therefore, in the present study we are dealing with the ordinary strange quark matter (SQM) [10,11].

The special problem in studying the EOS of ordinary quark matter is to treat quark confinement in a proper way. In the conventional standard approach an extra term, the famous bag constant B, is added to the energy density of the system, which provides a negative pressure to confine quarks within a finite volume, usually called a "bag." The quark mass is infinitely

large outside the bag, and a finite constant within the bag. A vast quantity of investigations have been performed within the framework of the bag model [12].

As is well known, however, particle masses vary with environment. Such masses are usually called effective masses. Effective masses of hadrons and quarks have been extensively discussed, e.g., within the Nambu-Jona-Lasinio model [13] and within a quasi-particle model [14]. In principle, the density dependence of quark masses should be connected to the in-medium chiral condensates [15,16].

Taking advantage of the density dependence, one can describe quark confinement without using the bag constant. Instead, the quark confinement is achieved by the density dependence of the quark masses derived from in-medium chiral condensates [17–19]. The two most important aspects in this model are the quark mass scaling [17,19] and the thermodynamic treatment [18,19]. Both aspects will be reviewed in this article.

In the present contribution, the transition from hadron phase (HP) to strange quark phase (SQP) in the inner core of a neutron star is investigated within the fully consistent nuclear and quark models. In the hadron sector we adopt the equation of state from Brueckner-Bethe-Goldstone (BBG) approach with three-body forces (TBF) [20–22]. This theory, being a completely microscopic approach, can easily incorporate degrees of freedom such as nucleon resonances [$\Delta(1232)$ or $N^*(1440)$], which are expected to appear at higher hadron densities. It is found that the mixed hadron-quark phase can occur, for reasonable values of the confinement parameter, a little above the normal saturation density, and can undergo the transition to pure quark matter at about five to six times the saturation. This result is quite different from the previous results from Nambu-Jona Lasinio (NJL) model in which the mixed quark phase cannot appear at neutron-star densities [23,24]. Afterwards, the influence of the mixed and quark phase on the structure of compact stars is discussed by solving the Tolman-Oppenheimer-Volkov (TOV) equation and extracting the mass-radius plots for neutron stars. Finally, it is shown that the transition to the deconfined phase turns out to be incompatible with the onset of kaon condensation.

II. EOS OF QUARK MATTER

SQM has been one of the hot topics in nuclear physics since the presentation of Witten's famous stability theory [10]. In many studies, the quark confinement was treated adopting the bag mechanism [11,25]. An alternative approach to obtain confinement is based on the density dependence of quark masses [26]. This mechanism has been extensively applied to investigate the properties of SQM [27–30]. In this section, we first give a short review on the two most important aspects and point out the main inconsistencies of the original model. Then we present a fully self-consistent thermodynamic treatment. The properties of SQM will be given in the new treatment. In the present article, however, the main application of the new approach is to study the phase transition in compact stars after

describing the Brueckner-Hartree-Fock (BHF) nuclear EOS in the next section.

A. Confinement by density-dependent masses

As mentioned above, the quark confinement in this model is achieved by the density dependence of quark masses. Therefore, the first important question is how to determine the quark mass scaling that can reasonably produce confinement. Originally, the interaction part of the quark masses was assumed to be inversely proportional to the density [26,27]. This linear scaling has been extensively applied to studying the properties of SQM [27–30]. There are also other mass scalings [31,32]. Their main drawback is that they are pure parametrizations without a convincing derivation. Therefore, a cubic scaling was derived based on the in-medium chiral condensates and linear confinement at both zero [17] and finite temperature [19]. This new scaling has been applied to investigating the viscosity of SQM and the damping time scale due to the coupling of the viscosity and r mode [33], the quark-diquark equation of state and compact star structure [34], the properties of strangelets versus the electric charge and strangeness [35], and the new solutions for CFL slets [36]. In the present article, we use the chirally determined quark mass scaling [17,19] to study the phase transition in neutron stars. For this we need a completely self-consistent thermodynamic treatment of the EOS of quark matter.

The thermodynamic treatment of the system with confinement via the density-dependent quark masses has been a long story. Originally, the thermodynamic formalism was regarded as the same with those of the constant-mass case [27]. In this first treatment, the internal pressure cannot be zero, and the properties of SQM were rather different from those in the bag model. But it was later pointed out that the difference was caused by the incorrect thermodynamic treatment [28]. It was found that an additional term is to be added to the pressure and energy expressions [28]. This second treatment makes it possible that SQM could be self-bound. However, two serious problems came out: one is the unreasonable vacuum limits and the other is the discrepancy between the energy minimum and zero pressure. It was shown that the added term in the pressure, due to the density dependence of quark masses, should not be appended to the energy. After discarding this term in the energy while keeping it in the pressure, the two inconsistencies mentioned above were immediately removed [18]. This third treatment has recently been extended to finite temperature [19]. The thermodynamic formalism in Ref. [18] was also adopted in Ref. [30], though a different quark mass scaling was used there.

A common feature of the last two thermodynamic treatments [18,19,28], as well as other recent references using this model [30], is that they all regard the thermodynamic potential as the same form with that of a Fermi gas. Because of the additional term, the pressure becomes obviously not equal to the minus thermodynamic potential density, contradicting the thermodynamic equality $P = -\Omega$ for a homogeneous system. One can also easily check that the fundamental differentiation equality $dE = \sum_i \mu_i dn_i$ for homogeneous

systems at zero temperature was not fulfilled in the mentioned references.

In the rest of this section, we will present a fully self-consistent thermodynamic treatment of the confinement by density-dependent mass model (CDDM).

B. Self-consistent thermodynamics in CDDM

Let us consider a quark model with three flavors. Denoting the Fermi momentum in the phase space by ν_i, the particle number densities can then be expressed as

$$n_i = g_i \int \frac{d^3\mathbf{p}}{(2\pi\hbar)^3} = \frac{g_i}{2\pi^2} \int_0^{\nu_i} p^2 \, dp = \frac{g_i \nu_i^3}{6\pi^2}, \qquad (1)$$

and the corresponding energy density as

$$E = \sum_i \frac{g_i}{2\pi^2} \int_0^{|\nu_i|} \sqrt{p^2 + m_i^2} \, p^2 \, dp. \qquad (2)$$

Equations (1) and (2) are familiar expressions, where the summation index goes over all considered particle types. To let the model be valid for both particles and antiparticles, the particle number density, or accordingly the Fermi momentum, is formally assumed to be negative for antiparticles. Therefore, in the upper limit of the integration, the absolute value has to be taken.

If the particle masses m_i are constant, the relation between the Fermi momenta ν_i and the chemical potentials μ_i is

$$\nu_i = \sqrt{\mu_i^2 - m_i^2} \quad \text{or} \quad \mu_i = \sqrt{\nu_i^2 + m_i^2}. \qquad (3)$$

As is well known, however, the quark mass depends on density and temperature. In principle, the quark mass scaling should be determined from QCD, which is obviously impossible presently. Based on the in-medium chiral condensates, a cubic scaling was derived at zero temperature [17], and it has been recently extended to finite temperature [19]. At zero temperature, we have the simple cubic scaling

$$m_q = m_{q0} + \frac{D}{n^z}, \qquad (4)$$

where m_{q0} is the quark current mass, n is the total baryon number density, the exponent of density is $z = 1/3$ [17], and the constant D is to be discussed a bit later.

In the following, we show that the density dependence of particle masses will modify the Fermi momentum, i.e., the relation in Eq. (3) for free-particle systems should be modified to include interactions. In fact for the quark flavor i we have

$$\mu_i = \left.\frac{dE}{dn_i}\right|_{\{n_{k\neq i}\}} = \frac{\partial E_i}{\partial \nu_i}\frac{d\nu_i}{dn_i} + \sum_j \frac{\partial E}{\partial m_j}\frac{\partial m_j}{\partial n_i}. \qquad (5)$$

Because the quark masses are density dependent, the derivatives generate an additional term with respect to the free Fermi gas model. We get

$$\mu_i = \frac{n_i}{|n_i|}\sqrt{\nu_i^2 + m_i^2} + \sum_j |n_j|\frac{\partial m_j}{\partial n_i} f\left(\frac{\nu_j}{m_j}\right), \qquad (6)$$

where

$$f(x) \equiv \frac{3}{2x^3}\left[x\sqrt{1+x^2} - \ln\left(x + \sqrt{1+x^2}\right)\right]. \qquad (7)$$

The pressure is then given by

$$\begin{aligned} P &= -E + \sum_i \mu_i n_i \\ &= -\Omega_0 + \sum_{ij} n_i |n_j| \frac{\partial m_j}{\partial n_i} f\left(\frac{\nu_j}{m_j}\right), \end{aligned} \qquad (8)$$

with Ω_0 being the free-particle contribution:

$$\begin{aligned} \Omega_0 = -\sum_i \frac{g_i}{48\pi^2}&\left[\nu_i\sqrt{\nu_i^2 + m_i^2}\,(2\nu_i^2 - 3m_i^2)\right.\\ &\left.+ 3m_i^4 \operatorname{arcsinh}\left(\frac{\nu_i}{m_i}\right)\right]. \end{aligned} \qquad (9)$$

Due to the additional term in the chemical potential, the pressure also has an extra term. The inclusion of such a term guarantees that the Hughenoltz-Van Hove theorem is fulfilled in the calculations.

In the quasiparticle model [37], one also has an extra term. Because the quark masses there depend on chemical potentials, and the extra term is not used in the relation between the Fermi momenta and chemical potentials, an effective bag constant has to be added to the energy expression [14] to consider confinement.

In CDDM quark model, however, we no longer need a bag constant. Quark confinement is achieved automatically by the density dependence of quark masses or by the strong interaction between quarks. In fact, the exponent $z = 1/3$ in Eq. (4) is derived from the linear confinement interaction [17].

In the present model, the parameters are the electron mass $m_e = 0.511$ MeV; the quark current masses m_{u0}, m_{d0}, m_{s0}; and the confinement parameter D. Although the light-quark masses are not without controversy and remain under active investigations, they are very small, and so we simply take $m_{u0} = m_{d0} = 0$. The current mass of strange quarks is 95 ± 25 MeV according to the latest version of the Particle Data Group [38].

Conventionally, the stability of strange quark matter (SQM) is judged by the minimum energy per baryon [10,11,27,28]. If it is less than 930 MeV (the mass of ^{56}Fe divided by 56), then SQM is absolutely stable. If it is bigger than 930 MeV but less than 939 MeV (the mass of nucleons), then it is metastable. Otherwise, if it is larger than 939 MeV, SQM is unstable. However, for two-flavor quark matter, it should be no less than 930 MeV to not contradict standard nuclear physics. This is the Witten-Bodmer hypothesis [10,11].

In Fig. 1, we show the different regimes in the $\sqrt{D}$-m_{s0} plane. The area below the full line is forbidden where the energy per baryon of two-flavor quark matter is less than 930 MeV. Above the dotted line, the energy per baryon of SQM is more than 939 MeV, and thus SQM is unstable. The area bounded by the dotted and dashed lines is the metastable region where the energy per baryon is between 930 and 939 MeV. Only when the $(D^{1/2}, m_{s0})$ pair is in the range between the full and dashed lines, SQM can be absolutely
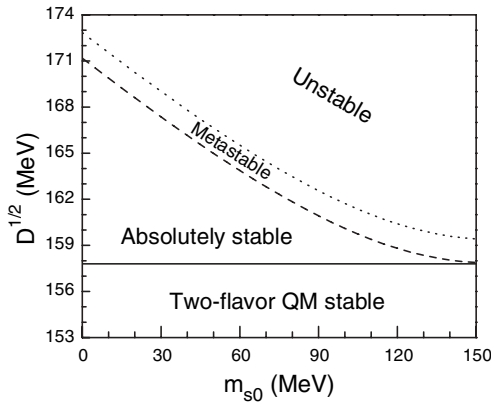
FIG. 1. Confinement constant range determined by stability arguments. SQM is absolutely stable only in the region bounded by the full and dashed lines.

stable, i.e., its energy per baryon is less than 930 MeV. Therefore, the range of D values is vary narrow for a chosen m_{s0} value if the Witten-Bodmer hypothesis is correct. If we take the modest value $m_{s0} = 100$ MeV, for example, then $D^{1/2}$ is in the range of 158–160 MeV. The lower bound 158 MeV is obtained by taking $m_{u0} = m_{d0} = 0$. If m_{u0} and m_{d0} are given a small finite value, the lower bound can then be a little bit smaller, e.g., 156 MeV [18].

Unfortunately we presently do not have a definite conclusion on the stability of SQM, so we treat D as a free parameter. However, the first condition, i.e., D greater than about $(158 \text{ MeV})^2$, should always be satisfied. However, we can connect D to the pion mass m_π, pion decay constant f_π, pion-nucleon sigma term σ_N, string tension σ_0, and the vacuum chiral condensate $\langle \bar{q}q \rangle_0$ by [19]

$$D = \frac{3(2/\pi)^{1/3}\sigma_0 m_\pi^2 f_\pi^2}{-\sigma_N \sum_q \langle \bar{q}q \rangle_0}. \tag{10}$$

From the known range of the vacuum condensate, we can have an upper bound $(270 \text{ MeV})^2$. Therefore, $D^{1/2}$ should not be out of the range (156, 270) MeV.

C. Properties of strange quark matter

As usually done, we consider SQM as a mixture of u, d, s quarks and electrons. The relevant chemical potentials $\mu_u, \mu_d, \mu_s,$ and μ_e satisfy the weak-equilibrium condition

$$\mu_u + \mu_e = \mu_d, \tag{11}$$

$$\mu_d = \mu_s. \tag{12}$$

Because all particle masses do not depend on the density of electrons, i.e., $\partial m_j / \partial n_e = 0$, Eq. (6) gives

$$\mu_i = \sqrt{(\pi^2 n_i)^{2/3} + m_i^2} - \mu_I \tag{13}$$

with

$$\mu_I = -\frac{1}{3} \frac{\partial m_I}{\partial n_b} \sum_{j=u,d,s} n_j f\left(\frac{v_j}{m_j}\right) \tag{14}$$

for $i = u, d, s$ quarks and

$$\mu_e = \sqrt{(3\pi^2 n_e)^{2/3} + m_e^2} \tag{15}$$

for electrons.

In Eq. (14), m_I is the second term on the right-hand side of Eq. (4), so we have $\partial m_I / \partial n = -zD/n^{z+1} = -zm_I/n$. The pressure is then obtained from Eq. (8) as

$$P = -\Omega_0 + n_b \frac{dm_I}{dn_b} \sum_{j=u,d,s} n_j f\left(\frac{v_j}{m_j}\right). \tag{16}$$

Substituting these expressions into Eqs. (11) and (12), we have

$$\sqrt{(\pi^2 n_u)^{2/3} + m_u^2} + \sqrt{(3\pi^2 n_e)^{2/3} + m_e^2} = \sqrt{(\pi^2 n_d)^{2/3} + m_d^2}. \tag{17}$$

and

$$(\pi^2 n_d)^{2/3} + m_d^2 = (\pi^2 n_s)^{2/3} + m_s^2. \tag{18}$$

We also have the baryon number density

$$n = \tfrac{1}{3}(n_u + n_d + n_s) \tag{19}$$

and the charge density

$$Q_q = \tfrac{2}{3}n_u - \tfrac{1}{3}n_d - \tfrac{1}{3}n_s - n_e. \tag{20}$$

The charge-neutrality condition requires $Q_q = 0$.

For a given total baryon number density n, we can obtain the respective $n_u, n_d, n_s,$ and n_e by solving the four Eqs. (17), (18), (19), and (20). The chemical potentials $\mu_u, \mu_d, \mu_s,$ and μ_e can then be calculated by Eqs. (13) and (15). Therefore, the energy density of the quark matter is a function of the baryon number density n and the charge density Q_q, i.e., $E_q = E_q(n, Q_q)$ or

$$dE_q = \frac{\partial E_q}{\partial n}dn + \frac{\partial E_q}{\partial Q_q}dQ_q, \tag{21}$$

where the two partial derivatives, $\partial E_q/\partial n$ and $\partial E_q/\partial Q_q$, are called the baryon chemical potential and charge chemical potential, respectively. It can be easily shown that they are connected to the quark chemical potentials by

$$\frac{\partial E_q}{\partial n} = \mu_u + 2\mu_d, \quad \frac{\partial E_q}{\partial Q_q} = \mu_u - \mu_d. \tag{22}$$

In fact, according to the fundamental differentiation equality of thermodynamics at zero temperature, we have

$$dE_q = \mu_u dn_u + \mu_d dn_d + \mu_s dn_s + \mu_e dn_e. \tag{23}$$

However, we have $\mu_e = \mu_d - \mu_u, \mu_s = \mu_d, n_s = 3n - n_u - n_d,$ and $n_e = n_u - n - Q_q$ from Eqs. (11), (12), (19), and (20). Substituting these four equalities into Eq. (23) leads to $dE = (\mu_u + 2\mu_d)dn + (\mu_u - \mu_d)dQ_q$. Comparison of this with Eq. (21) immediately gives Eq. (22).

In Fig. 2, the quark fractions, i.e., $n_u/(3n)$, $n_d/(3n)$, $n_s/(3n)$, and the 10^4 times the electron number divided by the total quark number, $10000n_e/(3n)$, have been shown versus the baryon number density for $D^{1/2} = 160$ MeV and $m_{s0} = 80$ MeV. It is seen that the fraction of up quarks is nearly always one third, the fraction of down quarks increases rapidly with decreasing densities, while the fraction of strange quarks
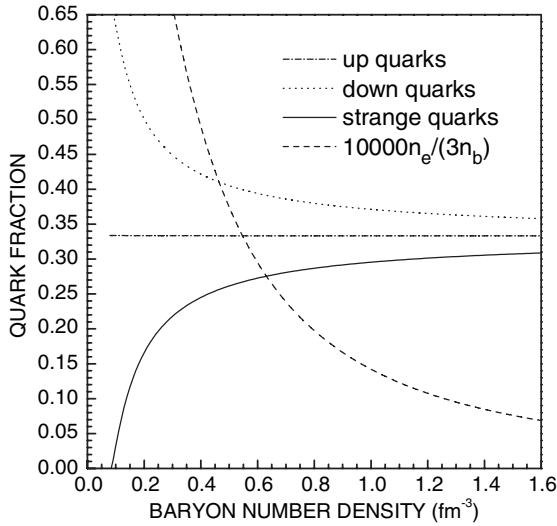
FIG. 2. Quark fraction vs. baryon number density for $D^{1/2} = 160$ MeV and $m_{s0} = 80$ MeV.

approaches to zero when the density decreases to a certain lower density.

To compare the relation between the Fermi momentum and chemical potential, we plot, in Fig. 3, the Fermi momentum of up (solid line), down (dotted line), and strange (dashed line) quarks, respectively, as a function of the corresponding quark chemical potential, in both the present model (lines with a solid circle) and the previous model (lines with an open circle). It is very obvious that the difference is very large, especially at comparatively lower densities. In both models, the Fermi momentum of up or down quarks is higher than that of strange quarks due to the fact that strange quarks are heavier than up or down quarks. For the same chemical potential, however, the Fermi momentum in the present model is generally bigger than that in the previous model, due to the quark-mass
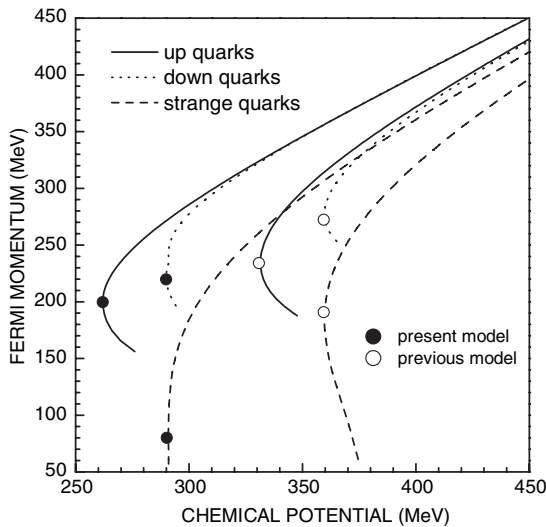

FIG. 3. Comparison between the Fermi momenta and chemical potentials. Parameters are the same as described in the caption for Fig. 2.
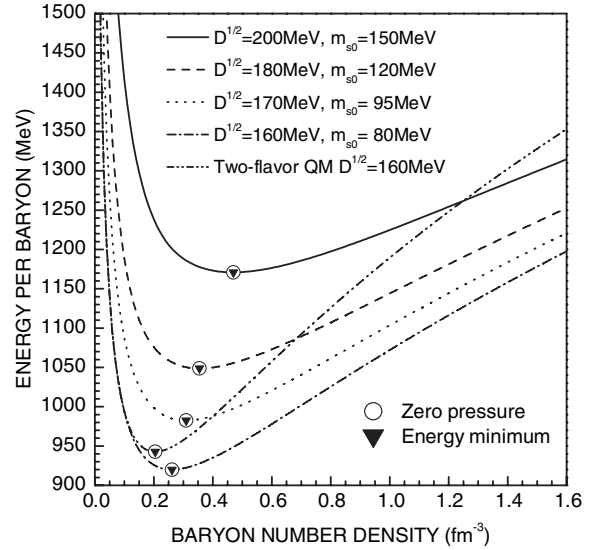

FIG. 4. Energy per baryon of quark matter in the present model. The parameter pair $(D^{1/2}, m_{s0})$ in MeV for the solid, dashed, dotted, and dash-dotted cures are (200,150), (180,120), (170,95), and (160,80), respectively. The dash-dot-dot line is for the two-flavor quark matter at $D^{1/2} = 160$ MeV. It is very obviously shown that the energy minimum, marked with a full triangle on each line, is located exactly at the same point of the zero pressure indicated by an open circle.

density dependence that reflects the strong interaction between quarks.

Figure 4 shows the energy per baryon of quark matter for different parameter sets in the present model. Each line has a minimum, corresponding to the lowest energy state (marked with a solid triangle). One can see that the pressure at this minimum is exactly zero. So this special point is marked with an open circle as well. At the same time, we also display the energy per baryon for the two-flavor quark matter by a dash-dot-dot line. We see that the two-flavor quark matter is less stable than SQM. Even for a smaller D value, e.g., $(160 \text{ MeV})^2$, its energy will finally exceed that of SQM for a bigger D with increasing densities.

In principle, the CDDM quark model contains more physics than the simple bag model. To demonstrate this we plot, in Fig. 5, the baryon chemical potential in CDDM with $D^{1/2} = 180$ MeV and $m_{s0} = 120$ MeV and in the bag model with $B^{1/4} = 180$ MeV. In CDDM, the baryon chemical potential decreases with decreasing density to a certain value depending on D and m_{s0}, then it increases very rapidly, i.e., it saturates at a definite density marked with a bullet. When the density is lower than the bullet, the derivative d^2E/dn^2 becomes negative, and so quark matter is unstable against phase separation and falls apart at lower densities. In the bag model, however, the baryon chemical potential is always a monotonic function of density, which means that quark matter does not fall apart at any lower densities. The velocity of sound has also been plotted on the right axis. We observe that it is, in the bag model, nearly the same as that of a noninteracting Fermi gas. But in CDDM, it decreases to zero with decreasing densities. At high densities, it
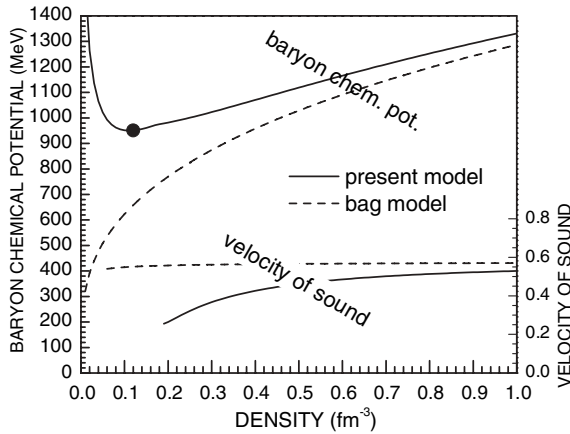
FIG. 5. The baryon chemical potential in CDDM ($\sqrt{D} = 180$ MeV, $m_{s0} = 120$ MeV) and in the bag model ($B^{1/4} = 180$ MeV). The former has a minimum at a lower density depending on the value of D and m_{s0}, whereas the latter is always a monotonic function of density. The velocity of sound in both models has also been given on the right axis.

becomes asymptotically identical to the ultrarelativistic limit, as expected.

D. Quark matter at finite temperature

Because the single particle energies depend on density and temperature via the quark masses, the thermal properties should be founded on the canonical ensemble, but, as is well known, the partition function is not easy to calculate. Therefore a different statistical procedure is usually adopted, which is based on the quasiparticle assumption. According to that the energy density is written as

$$E = \sum_i g_i \sum_{\mathbf{p}} \sqrt{p^2 + m_i^2}\, f_i(p, T), \qquad (24)$$

where the Fermi distribution function is

$$f_i(p, T) = \frac{1}{1 + e^{[\epsilon_i(p,T) - \mu_i]/T}}. \qquad (25)$$

If antiparticles are included, the sum must be extended to antiparticles for which μ_i must be replaced by $-\mu_i$. From the Landau definition of the single-particle energy extended to finite temperature, we have

$$
\begin{aligned}
\epsilon_i(p) &= \frac{\delta E}{\delta f_i(p, T)} \\
&= \sqrt{p^2 + m_i^2} + \sum_j g_j \frac{m_j f_j(p, T)}{\sqrt{p^2 + m_j^2}} \frac{\partial m_j}{\partial n_i} \\
&\equiv \varepsilon_i(p) - \mu_I, \qquad (26)
\end{aligned}
$$

where $\varepsilon_i(p) \equiv \sqrt{p^2 + m_i^2}$ is the dispersion relation of free particles. The extra term μ_I can be added to the chemical potential, so defining

$$\mu_i^* \equiv \mu_i + \mu_I. \qquad (27)$$

Accordingly, the net density of the particle type i is $n_i = g_i \sum_{\mathbf{p}} [f_i(p, T) - f_{\bar{i}}(p, T)]$, or, explicitly, we have

$$n_i = g_i \int_0^\infty \left\{ \frac{1}{1 + e^{[\varepsilon_i(p) - \mu_i^*]/T}} - \frac{1}{1 + e^{[\varepsilon_i(p) + \mu_i^*]/T}} \right\} \frac{p^2 dp}{2\pi^2}. \qquad (28)$$

Inverting this equation, one determines μ_i^* as a function of n_i so that the free energy density

$$F = \sum_i F_i(T, \mu_i^*, m_i) = \sum_i [F_i^+ + F_i^-] \qquad (29)$$

with

$$
\begin{aligned}
F_i^\pm = g_i \int_0^\infty \Bigg\{ &- T \ln\left[1 + e^{-(\sqrt{p^2 + m_i^2} \mp \mu_i^*)/T}\right] \\
&\pm \frac{\mu_i^*}{1 + e^{(\sqrt{p^2 + m_i^2} \mp \mu_i^*)/T}} \Bigg\} \frac{p^2 dp}{2\pi^2} \qquad (30)
\end{aligned}
$$

will be a function of respective particle densities instead of chemical potentials. One can then determine the real chemical potentials and pressure, according to the well-known relations

$$\mu_i = \frac{\partial F}{\partial n_i}, \qquad P = -F + \sum_i \mu_i n_i. \qquad (31)$$

These quantities will completely describe the thermal equilibrium of pure quark phase and the transition to the quark-hadron mixed phase. A more detailed analysis, where the thermodynamic formalism is developed to much more extent, is reported in Appendix A. In Ref. [19], the μ_i should be implicitly understood as μ_i^*.

In Fig. 6, we give the energy per baryon of SQM as a function of both density and temperature. The parameters used for this three-dimensional plot are $\sqrt{D} = 180$ MeV and $m_{s0} = 120$ MeV.
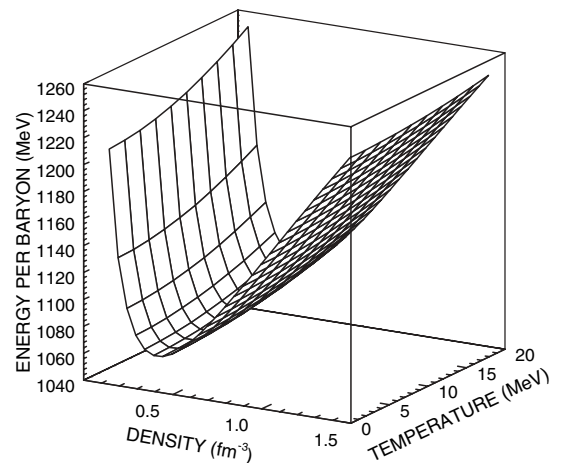

FIG. 6. Density and temperature dependence of the energy per baryon for the parameters $\sqrt{D} = 180$ MeV and $m_{s0} = 120$ MeV.

III. NUCLEAR MATTER IN BRUECKNER THEORY WITH THREE-BODY FORCES

The BBG theory is among the most advanced microscopic theories of nuclear matter. In recent years it was recognized that the three-body forces, which are expected to have a dominant role at high nuclear density, also affect the saturation point and, in fact, after including the three-body forces in the Brueckner theory, the empirical saturation properties are reproduced quite well [21,39]. In the neutron star interior, where high baryonic density values are reached, processes like the excitation of nucleon-antinucleon pairs (Z diagrams) and nucleonic resonances (together with the production of other hadrons) sizeably influence the two-body nuclear interaction. The former process involves the virtual excitation of negative energy states, which is absent from the standard Brueckner theory, and thus it represents a pure relativistic effect. From the comparison with the Dirac-Brueckner theory it turns out that it is by far the most important relativistic effect [39]. This process together with nucleon resonances can be incorporated in the interaction as medium virtual excitations in TBFs. One could guess that many body (more that three) forces are also important at high density as large as $\rho \approx 1$ fm^{-3}, but it is hard to imagine that pure baryon matter can exist at so high density. At lower density two and three-body forces are dominant because the hole line expansion is, roughly speaking, an expansion in density powers.

The global effect of TBFs at high density is strongly repulsive, leading to a remarkable increase of the maximum mass in the study of the neutron star structure. But also a correct estimate of the saturation point is important, because, as we will see below, in strongly asymmetric nuclear matter the threshold for the transition to mixed nucleon-quark phase can appear close to the saturation density. Therefore the corresponding EOS could be used as input for transport-model simulations of heavy-ion collisions, where strongly isospin-asymmetric systems are formed in central events.

A. BBG equations

The Brueckner theory extended to TBF is described elsewhere [20,21]. Here we simply give a brief review of the BHF approximation at finite temperature T [40–42]. The starting point is the reaction G matrix, which satisfies the BBG equation,

$$G(\omega, T) = \upsilon_{NN} + \upsilon_{NN} \sum_{k_1 k_2} \frac{|k_1 k_2\rangle Q_{k_1,k_2}(T)\langle k_1 k_2|}{\omega - \epsilon_{k_1}(T) - \epsilon_{k_2}(T)} G(\omega, T),$$

(32)

where $k_i \equiv (\vec{k}_i, \sigma_i, \tau_i)$, denotes the single-particle momentum, the z component of spin and isospin, respectively, and ω is the starting energy. The G matrix, the Pauli operator Q, and the single-particle energies $\epsilon_k(T) = k^2/2m + U_k(T)$ depend on the neutron and proton densities and temperature. The interaction υ_{NN} given by

$$\upsilon_{NN} = V_2^{\text{bare}} + V_3^{\text{eff}},$$

(33)

where V_2^{bare} is the bare two-body force (2BF) and V_3^{eff} is an effective 2BF derived by the average of the bare TBF on the third particle as follows

$$\langle \vec{r}_1 \vec{r}_2 | V_3^{\text{eff}}(T) | \vec{r}_1' \vec{r}_2' \rangle = \frac{1}{4} \text{Tr} \sum_n \int d\vec{r}_3 d\vec{r}_3' \phi_n^*(\vec{r}_3')[1 - \eta(r_{13}', T)]$$
$$\times [1 - \eta(r_{23}', T)] \times W_3(\vec{r}_1' \vec{r}_2' \vec{r}_3' | \vec{r}_1 \vec{r}_2 \vec{r}_3)$$
$$\times \phi_n(r_3)[1 - \eta(r_{13}, T)][1 - \eta(r_{23}, T)].$$

(34)

Because the defect function $\eta(r, T)$ is directly determined by the solution of the BBG equation [20], V_3^{eff} must be calculated self-consistently with the G matrix and the single-particle potential U_k on the basis of BBG equation. It is clear from Eq. (34) that the effective force rising from the TBF in nuclear medium is density and temperature dependent through the defect function. A detailed description and justification of the method can be found in Ref. [20], including a discussion on the averaging procedure. The validity of such a procedure has been numerically tested in the comparison between the BHF EOS plus Z diagrams with σ meson exchange and the Dirac-BHF EOS, which are expected to be equal. The calculation [39] gives an impressive agreement between the two EOS's, although the TBF due to the Z diagrams is averaged according to Eq. (34).

For V_2^{bare} we adopt the Argonne V_{18} two-body interaction [43]. The TBF is constructed from the meson-exchange current approach [20] and contains virtual particle [Δ and $N^*(1440)$] excitations and, in addition, relativistic effects induced by the excitations of particle-antiparticle pairs. This description of the interaction is not completely consistent because, in principle, the two and three body forces should be derived from the same meson parameters, but a recent calculation [39] replacing Argonne potential with Bonn potential [44] and the TBF built up with the Bonn meson parameters substantially leads to the same results.

B. Thermodynamics

Let us start with symmetric nuclear matter. In the BHF approximation, the thermodynamic potential can be written

$$\Omega_N = \Omega_N^0 + W_L,$$

(35)

$$\Omega_N^0 = -T \sum_k \ln\left[1 + e^{-(\epsilon_k - \mu)/T}\right],$$

(36)

$$W_L = -\frac{1}{2} \sum_k f_k(T) U_k(T),$$

(37)

where Ω_N^0 is the thermodynamic potential for a system of independent particles with the single-particle spectrum $\epsilon_k = \frac{\hbar^2 k^2}{2m} + U_k(T)$ and W_L is the sum of all linked cluster diagrams to the lowest order in the hole line expansion [40]. $U_k(T)$ is the self-consistent mean field,

$$U_k(T) = \sum_{k'} \langle kk' | G | kk' \rangle_A f_{k'}(T).$$

(38)

The finite temperature BHF approximation suffers from the same difficulty as any strongly interacting Fermi system.

The difficulty is the same as in the CDDM quark model, because in both cases the single-particle spectrum is density and temperature dependent. Whereas at $T = 0$ the density (or Fermi momentum) can be fixed, at $T > 0$ the role of density is taken by chemical potential μ (grand canonical ensemble), and one is forced to fix the chemical potential at each iteration due to the presence of the Fermi distribution $f_k(T) = \{1 + \exp([\epsilon_k(T) - \mu]/T)\}^{-1}$. Because this procedure does not converge [40], one should fix the density and invert the equation relating density and chemical potential,

$$\rho = \frac{1}{V} \sum_k f_k(T) - \left(\frac{\partial W_L}{\partial \mu}\right)_T, \qquad (39)$$

which is not a viable task. The usual approximation is to drop out the derivative in the previous equation, which corresponds to the quasiparticle approximation above discussed within the CDDM quark model. In so doing, the resulting $\tilde{\mu}$ looses its meaning of chemical potential. In this approximations the energy and entropy densities are given by:

$$E_N = \frac{1}{V} \sum_k f_k(T) \left[\frac{\hbar^2 k^2}{2m} + U_k(T)\right], \qquad (40)$$

$$S_N = -\frac{1}{V} \sum_k \{f_k(T) \ln f_k(T) + [1 - f_k(T)] \ln[1 - f_k(T)]\}. \qquad (41)$$

After one calculates $\tilde{\mu}$ in terms of ρ, the thermodynamics is developed from the free energy density $F_N(\rho, T) = E_N(\rho, T) - T S_N(\rho, T)$. The free energy per particle, calculated from BHF approximation, is depicted in Fig. 7. Due to the difficulty of extending the BHF code to very high temperature an extrapolation from the real numerical results to high T has been performed adopting the so called frozen approximation based on T-independent single-particle spectrum, i.e., the latter is frozen at $T = 0$. This turns out to be a good approximation up to $\sim$10–20 MeV [45].

The relevant thermodynamical quantities, i.e., chemical potentials and pressure, are derived from free energy as follows

$$\mu = \left.\frac{\partial F_N}{\partial \rho}\right|_T, \qquad P = \rho^2 \frac{d(F_N/\rho)}{d\rho}. \qquad (42)$$
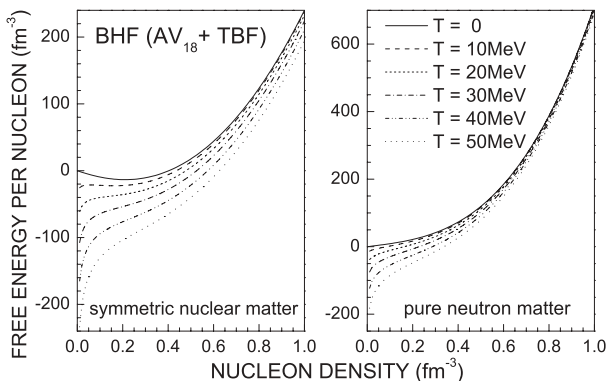

FIG. 7. Isotherms of symmetric nuclear matter (left side) and pure neutron matter (right side) as a function of the nucleon density at different temperature.

Let us consider asymmetric nuclear matter with baryon density $\rho = \rho_n + \rho_p$ and asymmetry parameter $\beta = (\rho_n - \rho_p)/\rho$, where ρ_n (ρ_p) is the neutron (proton) density. The baryon chemical potentials can be expressed as

$$\mu_n = \left(\frac{\partial F_N}{\partial \rho_n}\right)_{T, \rho_p}, \qquad \mu_p = \left(\frac{\partial F_N}{\partial \rho_p}\right)_{T, \rho_n}, \qquad (43)$$

where F_N is the free energy density.

Assuming the parabolic law for the latter, we get the simple expression for the chemical momentum isotopic shift

$$\mu_n - \mu_p = 4\beta F_{\text{sym}}(\rho, T), \qquad (44)$$

where F_{sym} is the symmetry free energy density. The parabolic law is well satisfied at low density, but at high density additional terms of the β expansion must be considered.

In neutron star inner core nuclear matter is supposed to be in β equilibrium under the condition of charge neutrality. Assuming that only electrons are present (the muon contribution is negligible), the two preceding conditions require

$$\mu_e = \mu_n - \mu_p, \qquad (45)$$

$$Q_N = \rho_p - \rho_e. \qquad (46)$$

Q_N is the net charge density of nuclear matter. It is zero for pure neutral nuclear matter. For a given set of (ρ, Q_N), we can solve the chemical potentials μ_n, μ_p, and μ_e from the above equations. Then all other quantities can be obtained for a fixed temperature. In other words, all thermodynamic quantities can be regarded as a function of the nucleon density ρ, charge density Q_N, and temperature T. At zero temperature, for example, the energy density can be regarded as a function of ρ and Q_N, i.e., $E_N = E_N(\rho, Q_N)$. With a similar approach as in the preceding section to obtain Eq. (22), we can easily show that the baryon chemical and charge chemical potentials of nuclear matter can be expressed as

$$\frac{\partial E_N}{\partial \rho_n} = \mu_n, \qquad \frac{\partial E_N}{\partial Q_N} = \mu_p - \mu_n. \qquad (47)$$

The system turns out to be in a strongly isospin asymmetric state. The isotherms of free energy and pressure of nuclear matter in β equilibrium are shown in Fig. 8.

IV. PHASE DIAGRAM STRUCTURE AT ZERO AND FINITE TEMPERATURES

Let us study the nuclear matter, consisting of nucleons and electrons, in equilibrium with a gas of u, d, s quarks and electrons. According to Glendenning [46,47], we assume the total charge conservation, in addition to total baryon and energy conservation. Now we first consider the case of zero temperature and then extend to finite temperatures.

The conservation laws can be imposed by introducing the quark fraction χ defined as

$$\chi \equiv V_q/V. \qquad (48)$$

where V is the total volume and V_q is the volume occupied by quarks. Then the total baryon density is
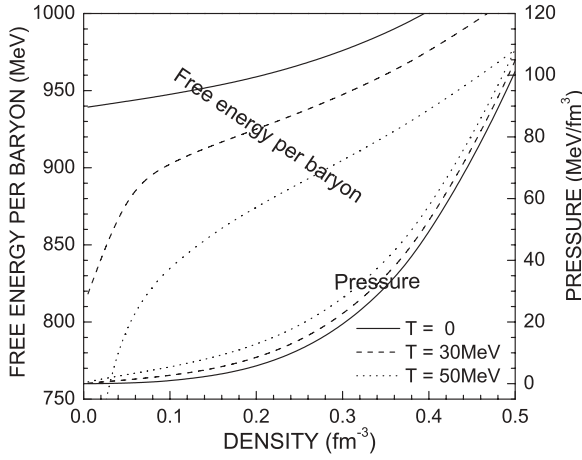
$$\rho_t = (1 - \chi)\rho + \chi n, \qquad (49)$$

FIG. 8. The free energy per baryon (left y axis) and pressure (right y axis) of nuclear matter in β equilibrium. Three values of the temperature are considered.

the total electric charge is

$$Q_t = (1 - \chi)Q_N + \chi Q_q, \tag{50}$$

and the total energy density is

$$E_t = (1 - \chi)E_N + \chi E_q, \tag{51}$$

where ρ, Q_N, and E_N are, respectively, the baryon number density, electric charge density, and energy density of nuclear matter, whereas n, Q_q, and E_q are the corresponding quantities of quark matter. E_N is a function of ρ and Q_N, E_q is a function of n and Q_q, i.e., $E_N = E_N(\rho, Q_N)$, $E_q = E_q(n, Q_q)$. Differentiating Eq. (51), one obtains

$$dE_t = (1 - \chi)\left(\frac{\partial E_N}{\partial \rho}d\rho + \frac{\partial E_N}{\partial Q_N}dQ_N\right)$$
$$+ \chi\left(\frac{\partial E_q}{\partial n}dn + \frac{\partial E_q}{\partial Q_q}dQ_q\right) + (E_q - E_N)d\chi. \tag{52}$$

However, differentiating Eqs. (49) and (50) at a given pair of ρ_t and Q_t, we have

$$(1 - \chi)d\rho = (\rho - n)d\chi - \chi dn, \tag{53}$$

$$(1 - \chi)dQ_N = (Q_N - Q_q)d\chi - \chi dQ_q. \tag{54}$$

To minimize E_t, we substitute Eqs. (53) and (54) into Eq. (52). Then setting $dE_t = 0$, we find

$$\frac{\partial E_N}{\partial \rho} = \frac{\partial E_q}{\partial n}, \quad \frac{\partial E_N}{\partial Q_N} = \frac{\partial E_q}{\partial Q_q}, \quad P_N = P_q, \tag{55}$$

where

$$P_N = -E_N + \rho\frac{\partial E_N}{\partial \rho} + Q_N\frac{\partial E_N}{\partial Q_N}, \tag{56}$$

$$P_q = -E_q + n\frac{\partial E_q}{\partial n} + Q_q\frac{\partial E_q}{\partial Q_q}. \tag{57}$$

The conditions in Eq. (55) are nothing but the Gibbs ones, i.e., the baryon chemical potential, the charge chemical potential, and the pressure in nuclear and quark matter should be equal to each other to minimize the total energy of the mixed phase.

In the previous two sections, we have linked the baryon chemical potential and charge chemical potential to the respective constituent particle chemical potentials in Eqs. (22) and (47). As application of these equalities, we immediately see that the first two equations in (55) are equivalent to

$$\begin{array}{ll} \mu_n = \mu_u + 2\mu_d, & \mu_u = (2\mu_p - \mu_n)/3, \\ \mu_p = 2\mu_u + \mu_d. & \text{or} \quad \mu_d = (2\mu_n - \mu_p)/3. \end{array} \tag{58}$$

In general, all other chemical potentials in quark sector can be related to μ_u and μ_d, e.g., $\mu_s = \mu_d$, $\mu_e = \mu_d - \mu_u$. Similarly, all chemical potentials in nuclear sector can be linked to μ_n and μ_p, e.g., $\mu_e = \mu_n - \mu_p$. Therefore, Eq. (58) means that we can choose either (μ_u, μ_d) or (μ_n, μ_p) as the two independent chemical potentials. The latter can then be determined by solving the charge neutrality equation and the pressure balance equation for a given total baryon number or a given quark fraction.

At finite temperature, we similarly have the phase equilibrium condition

$$P_N = P_q \quad \text{(mechanical)}, \tag{59}$$

$$\mu_N = \mu_q \quad \text{(chemical)}, \tag{60}$$

$$T_N = T_q \equiv T \quad \text{(thermodynamical)}. \tag{61}$$

The condition in Eq. (61) tells us only that the temperature in nuclear and quark sectors are equal, so we have a common temperature T. The chemical equilibrium condition in Eq. (60) is equivalent to that in Eq. (58). Therefore, we still have only two independent chemical potentials. For a given total density ρ_t at a fixed temperature T, the two independent chemical potentials and the quark fraction χ can then be determined by solving the three equations in Eqs. (49), (50) with $Q_t = 0$, and (59).

Similar to the case at zero temperature, the lower critical density ρ_{c1}, which separates the nuclear and mixed phases, is defined by $\chi = 0$, whereas the critical density ρ_{c2} between the mixed and quark phases is determined by $\chi = 1$.

In Fig. 9, we display, for the parameter $\sqrt{D} = 170$ MeV, the density dependence of the energy per baryon in pure nuclear matter, in pure quark matter, and in the mixed phase. The quark fraction has also been depicted in the right y axis. In Fig. 10 the corresponding pressure is reported. It is seen that the nuclear matter is the most favorite phase at lower densities, and the quark matter is the most stable phase at higher densities, whereas at intermediate densities, the mixed phase has the lowest energy.

The quark baryon number density n and nuclear density ρ are also plotted on the right axis of Fig. 10. We see that the quark density is always higher than the nuclear density. The transition from hadron phase to mixed phase occurs at the density a bit less than 0.15 fm^{-3}, well below the saturation density. But it is hard to observe in terrestrial laboratories, because the nuclear matter so far realized in exotic nuclei or heavy-ion collisions is much less neutron rich. The transition from mixed phase to pure quark phase occurs at the total density $\rho_t = 0.85$ fm^{-3}, where the nuclear density is only $\rho = 0.64$ fm^{-3}. The density range of the mixed phase depends only slightly on the temperature, at least in the temperature range of interest in neutron stars.
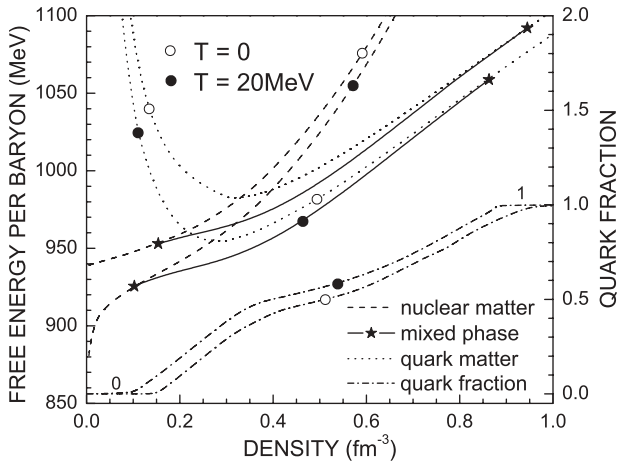
FIG. 9. The free energy per baryon as a function of density in the nuclear (dashed curves), mixed (solid), and quark phase (dotted). The quark fraction is also shown on the right axis with dash-dotted lines. The curves with an open circle are at zero temperature, whereas those with a full circle are for the temperature $T = 20$ MeV.

The critical densities depend on the parameter D. In the left panel of Fig. 11, both nuclear critical density (the solid line, separating the pure nuclear phase and the mixed phase) and the quark critical density (the dashed line, delimiting the pure quark phase) are displayed as a function of $D^{1/2}$. If $D^{1/2} < 161.6$ MeV, the two critical densities approach zero, and accordingly SQM is absolutely stable. When 161.6 MeV $< D^{1/2} < 162.5$ MeV, the mixed phase can exist at any lower densities. The nuclear matter is more stable at lower densities only when $D^{1/2} > 162.5$ MeV. If we have only two flavor quarks in the quark sector, the critical densities are usually higher. In the same panel we also plot the lower critical density for the two-flavor case. Because we know in our real world the two-flavor quark matter does not exist below the saturation density, $D^{1/2}$ should be on the right of the first full
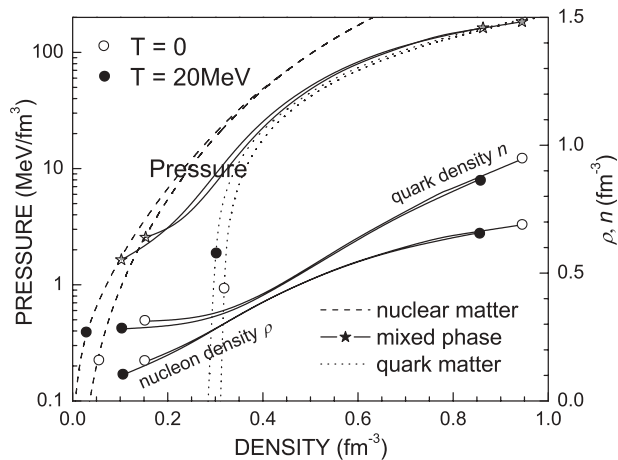

FIG. 10. The pressure in nuclear (dashed curve), mixed (solid), and quark phase (dotted) vs. density at temperature $T = 0$ (cures with an open circle) and 20 MeV (cures with an solid circle). The nuclear density ρ and the quark density n in the mixed phase are also shown on the right axis.
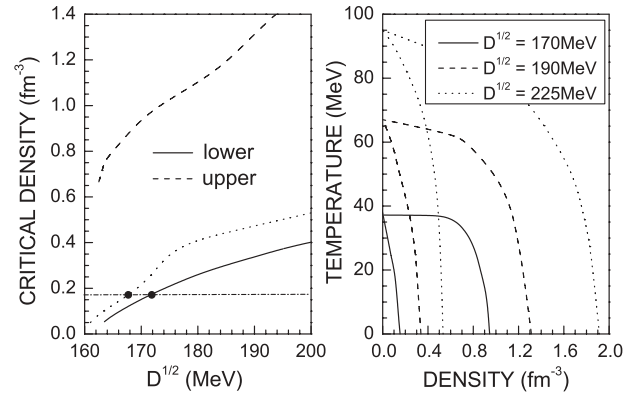

FIG. 11. (Left panel) The critical density of nuclear matter to quark matter as a function of the confinement parameter D. The horizontal line is the nuclear saturation density. The dotted line is the quark critical density in the case of two-flavor quark system. (Right panel) Phase diagram for three values of the confinement parameter and $m_{s0} = 95$ MeV.

dot at $D^{1/2} \approx 168$ MeV (the intersection of the dotted and dot-dashed lines) in Fig. 11. However, to let SQM have a chance to appear below the saturation density, $D^{1/2}$ should be on the left of the second full dot where $D^{1/2} = 171.3$ MeV. In plotting Figs. 9 and 10, we adopt $D^{1/2} = 170$ MeV. The temperature dependence of the lower and higher critical densities is also plotted in Fig. 11 (right panel). The two lines at fixed D mark the boundaries of the three phases.

V. PROPERTIES OF HYBRID STARS

With the equation of state that has the mixed and/or quark phase derived in Sec. IV, we are ready to study the structure of hybrid stars by solving the Tolman-Oppenheimer-Volkov equation

$$\frac{dP}{dr} = -\frac{GmE}{r^2} \frac{(1 + P/E)(1 + 4\pi r^3 P/m)}{1 - 2Gm/r}, \quad (62)$$

where $G = 6.707 \times 10^{-45}$ MeV^{-2} is the gravitational constant, r is the distance from the center of the star, and $E = E(r)$ and $P = P(r)$ are the energy density and pressure at the radius r, respectively. The subsidiary condition is

$$dm/dr = 4\pi r^2 E, \quad (63)$$

with $m = m(r)$ being the mass within the radius r.

At variance with pure nuclear or quark stars, a hybrid star contains pure quark matter in the core, pure nuclear matter near the outer part, and, in between, a mixed phase of the quark and nuclear matter. In this case, therefore, we must use the EOS in the whole density range.

The resulting gravitational mass for the hybrid star is plotted in Fig. 12, as a function of both radius and central density for four values of the confinement parameter $D^{1/2}$ of 170, 180, 190, 200 MeV. The main effect of the phase transition is, as expected, a large reduction of the maximum mass due to softening of the EOS. Concerning the confinement parameter D, we observe a slight decrease of the maximum
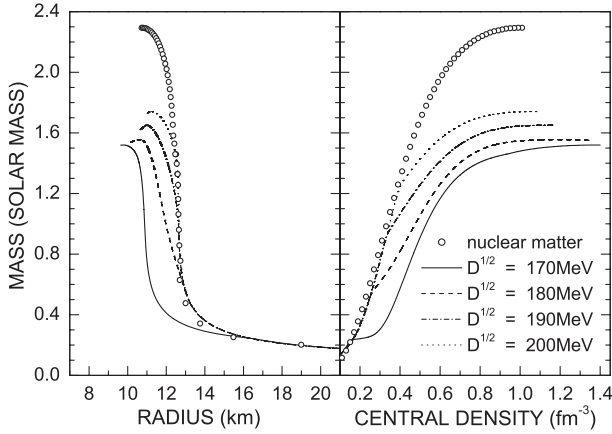
FIG. 12. Mass-radius relation of hybrid stars at $m_{s0} = 95$ MeV for four values of the confinement parameter $D^{1/2}$ of 170, 180, 190, 200 MeV.

mass when the D value becomes smaller, from $1.74 M_\odot$ at $D^{1/2} = 200$ MeV down to 1.6, 1.55, $1.52 M_\odot$ corresponding to $D^{1/2} = 190, 180, 170$ MeV. This can be easily understood in this way: because the quark phase occurs at a lower density for smaller values of D, sometimes even less than the nuclear saturation density (for example only 0.15 fm^{-3} for $D^{1/2} = 170$ MeV), then the quark population of the star would be more numerous, because the stronger softening of the EOS may only support less gravitational mass. In particular, the most favorable case of $D^{1/2} = 180$ and 190 MeV, when the quark confinement appears at around $2\rho_0$ consistent with the heavy-ion experiment, the predicted maximum mass can match very well the S branch of neutron stars mentioned by Haensel *et al*. with an error less than 5% [2].

To study the temperature effect on the mass of hybrid stars, in Fig. 13 we plot the star mass against the star radius or central density at $T = 0$ and $T = 20$ MeV. It is seen that the temperature influence on the maximum mass is very limited. Otherwise the effect is a quite strong increase of the NS radius for a fixed amount of gravitational mass. But the larger the mass the smaller the radius variation, which is similar to a few other calculations [48].
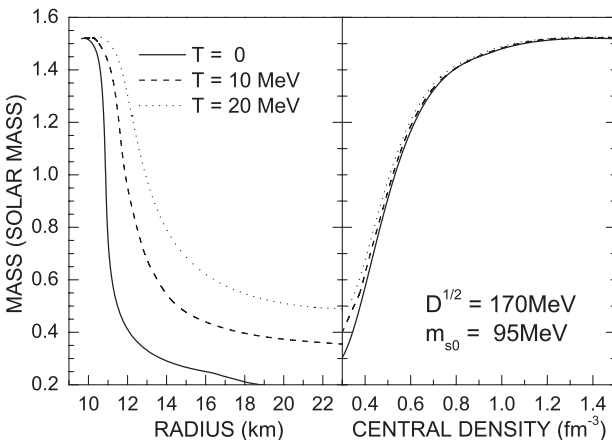

FIG. 13. Temperature effect on the mass-radius relation of hybrid stars.

A. Kaon condensation

The condensation of K^- mesons in neutron stars is widely discussed in the literature (see Refs. [49,50] and references therein). In dense matter, the condensation of K^- mesons is originated by the reaction

$$e^- \rightarrow K^- + \nu. \tag{64}$$

If the effective mass of the K^- drops below the chemical potential of the electron, this reaction becomes possible in dense matter, indicating the presence of kaon condensation. Because almost all the studies of kaon medium properties [51] suggest the consistent picture that the attraction from nuclear matter would bring the K^- mass down, so the threshold condition for the onset of K^- condensation $\mu_e = m_K^*$, which follows from Eq. (64), could be fulfilled in the center of neutron stars [51] at $\rho \gtrsim 3\rho_0$. However, the deconfinement phase transition from the hadronic phase to the quark phase occurs also at rather low density, which leads to the onset of mixed phase in neutron stars. It is then very interesting to explore how the quark deconfinement affects the K^- condensation threshold.

We take the antikaon dispersion relation constrained by the heavy-ion data as empirical indication of an attractive antikaon potential in dense matter [51] and combine this with the BHF model of nuclear matter together with the above quark model without bag constant to calculate the effective kaon mass in hybrid stars. The result is illustrated in Fig. 14, where the effective kaon mass and the electron chemical potential are shown in normal nuclear matter and especially in mixed phase for three selected values of the confinement parameter D. One sees that in normal nuclear matter, K^- medium mass decreases with increasing density and meets the electron chemical potential at ~ 0.6 fm^{-3} (the solid bullet in Fig. 14), so the kaon condensation would be present for sure in this case. However, once the quark phase sets in at the total density of 0.26, 0.4, 0.53 fm^{-3}, respectively, for
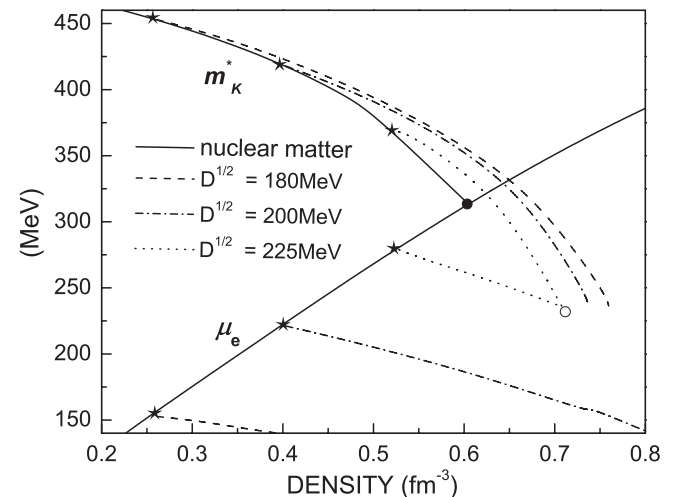

FIG. 14. The effective kaon mass and the electron chemical potential are shown in normal nuclear matter and also in mixed phase at $m_{s0} = 95$ MeV for three selected values of the confinement parameter $D^{1/2}$ of 180, 200, 225 MeV.

$D^{1/2} = 180, 200, 225$ MeV, the decreasing speed of the kaon effective mass in the matter slows down a little bit. In addition, more conclusively, the electron population begins to decrease instead, because the electric charge neutrality can be achieved more efficiently through the charged quarks themselves. As a result the threshold condition of K^- condensation is much more difficult to satisfy, unless the confinement parameter D is chosen to be extremely high (at least $D^{1/2} = 225$ MeV) when the presence of quark phase is pushed to very high densities, then one may expect that m_K^* can finally equal to μ_e (which is indicated with a circle). Those high values of D may even not be realistic, therefore we would like to conclude that the inclusion of quark phase may make the kaon condensation impossible in neutron stars or at least hinder it very strongly.

VI. DISCUSSION AND CONCLUSIONS

In this article the neutron star inner structure was studied. The lack of strong observational constraints demands for sophisticated models of the NS composition and interaction mechanisms. In this study we included only baryons and quarks in equilibrium with leptons and kaons. Because high baryon densities are reached in the NS interior, $N\bar{N}$ and nucleonic excitations are expected to play a major role. Their effects can be incorporated in a three-body force. The baryon EOS in weak coupling equilibrium with electrons was derived within the BBG theory suitably extended so to include the three-body force. In the quark sector, we adopted the semiphenomenological CDDM quark model, which exhibits a confinement mechanism alternative to the crude MIT bag model. Furthermore, in contrast with the extension of the MIT model, where the density dependence is introduced artificially [52], the CDDM quark model shapes its density dependence in agreement with chiral requirements [15,16].

Hadrons and quarks in β equilibrium were considered at zero and finite temperature. Because typical temperatures of protoneutron stars are as high as 40 MeV and beyond, rigorous thermodynamic potentials have to be derived. This was possible with the CDDM quark model because of its simplicity, whereas some approximations are needed to calculate the hadron phase in the Brueckner theory. The latter is still a main drawback of the finite temperature microscopic theory of strongly interacting Fermi systems.

The transition from the low-density hadron phase to the high-density quark phase in β equilibrium was studied under the Glendenning hypothesis of total charge neutrality. The Gibbs construction enabled to follow the evolution of the mixed hadron-to-quark phase, varying the temperature T and the confinement parameter D. The EOS, in terms of pressure, energy density, and chemical composition, was constructed as a function of T and D. Moreover, the phase diagram T-D was also depicted. The transition density from hadron to mixed phase is strongly dependent on the confinement parameter and, for a small-enough D, it becomes lower than the nuclear saturation density. However, at that point nuclear matter is so strongly neutron rich that it hard to imagine that it can be observed in terrestrial laboratory experiments. At high temperature the transition density is comparatively smaller.

The TOV equations were solved in the above-discussed model of neutron stars. The transition to quark matter produces a strong reduction of the maximum mass, from $M = 2.3 M_\odot$ to $1.5 M_\odot$ for the lowest value of the confinement parameter D, but the corresponding radius is not changed, being in both cases about 10 km. The other M-R configurations lie in a range $R \simeq 10$–13 km, depending on the value of D. With increasing D, the maximum mass increases from 1.5 to 1.7 solar masses. Other quark models have been adopted to describe the NS transition to a deconfined phase (see, for instance, Refs. [23,24,48]). Except for the Nambu-Jona Lasinio model that exhibits instability of neutron stars [24], the other models point to a softening of the EOS of nuclear matter. The MIT model, with a density-dependent bag constant, predicts a β-stable quark phase quite similar to that of our model [48], but the comparison on the NS structure turns out to be difficult, because in that calculation the transition to quark phase is built on top of hyperonized nuclear matter.

The effect of temperature on the maximum mass is negligible up to $T = 20$ MeV, but as expected the heated system can support much less gravitational mass in the same volume for all M-R configurations. Thus, an evolutionary study of isolated neutron stars would show a strong compression from the newborn phase to the long era phase as fast as the star cools down from 40 MeV to approximately zero.

Beyond the confinement parameter, the transition to quark phase is interrelated to other properties, in particular the possible onset of kaon condensation. In our analysis we concluded that the quark phase could not be compatible with the kaon condensation in neutron stars, or at least could hinder it very strongly.

The model developed in this article misses some important aspects. The first one is the effect of neutrinos. Neutrinos play the major role in new born neutron stars, when they are still trapped in the interior. In this case the neutronization process is still hindered and the EOS is that of symmetric nuclear matter. Moreover, the onset of kaon condensation is shifted to higher densities [53] and probably kaons have no more any chance to compete with quarks.

The second one is the inclusion of hyperons and their competition with other mechanisms such as kaon condensation. In Refs. [48] the hybrid stars are studied by including hyperons in the hadron phase, which makes the hadron EOS very soft and brings the maximum mass to $M = 1.25 M_\odot$. The introduction of the quark phase rises up again the maximum mass to $1.5 M_\odot$, a value that is consistent with our prediction without hyperons. However, the appearance of hyperons depends heavily on the threshold of kaon production. Therefore the interplay between hyperons and kaons turns out to be quite important and deserves additional investigation, as soon as more reliable empirical inputs will be available, especially on the hyperon-nucleon and hyperon-hyperon interaction.

ACKNOWLEDGMENTS

APPENDIX: THERMODYNAMICS WITH CONFINEMENT BY THE DENSITY DEPENDENCE OF QUARK MASSES

We begin with the fundamental thermodynamic differentiation relation $d(VE) = Td(VS) - PdV + \sum_i \mu_i d(Vn_i)$, where S is the entropy density and (anti-)particles are assumed to be uniformly distributed in a volume V. By using the free energy density $F = E - TS$, it becomes $d(VF) = -VSdT - PdV + \sum_i \mu_i d(Vn_i)$, or, equivalently, $dF = -SdT + (-P - F + \sum_i \mu_i n_i)dV/V + \sum_i \mu_i dn_i$. Because of the uniformity, the free energy density has nothing to do with the volume. We thus have

$$P = -F + \sum_i \mu_i n_i, \tag{A1}$$

$$dF = -SdT + \sum_i \mu_i dn_i. \tag{A2}$$

At finite temperature, we should consider both particles and antiparticles, and particles/antiparticles are not always located below the Fermi energy. Therefore, the net particle number densities can be expressed as

$$n_i = n_i(T, \mu_i^*, m_i) = n_i^+ - n_i^-, \tag{A3}$$

where the superscript $+$ indicates particles and superscript $-$ signifies antiparticles:

$$n_i^{\pm} = g_i \int_0^{\infty} \frac{1}{1 + e^{(\sqrt{p^2 + m_i^2} \mp \mu_i^*)/T}} \frac{p^2 dp}{2\pi^2}. \tag{A4}$$

In Eqs. (A4) and (A3), μ_i^* are effective chemical potentials of respective particles. If quark densities are not density and/or temperature dependent, μ_i^* are nothing but the actual chemical potentials. In our present case, however, quark masses depend on both density and temperature to include the strong interaction between quarks. Therefore, the real chemical potentials should be derived according to fundamental thermodynamic laws.

Equation (A3) gives, implicitly, μ_i^* as a function of T, n_i, and m_i, i.e.,

$$\mu_i^* = \mu_i^*(T, n_i, m_i). \tag{A5}$$

To determine the thermodynamic properties, we need to give a characteristic function. At zero temperature, we use the energy density in Eq. (2) due to zero entropy. Now the temperature T and the densities n_i are chosen as the independent system variables; we should, therefore, choose the free energy in Eq. (29) as the characteristic function.

Differentiation of Eq. (29) gives

$$dF = \sum_i \left[\left(\frac{\partial F_i}{\partial T} + \frac{\partial F_i}{\partial \mu_i^*} \frac{\partial \mu_i^*}{\partial T} \right) dT \right.$$
$$\left. + \frac{\partial F_i}{\partial \mu_i^*} \frac{\partial \mu_i^*}{\partial n_i} dn_i \left(\frac{\partial F_i}{\partial m_i} + \frac{\partial F_i}{\partial \mu_i^*} \frac{\partial \mu_i^*}{\partial m_i} \right) dm_i \right]. \tag{A6}$$

Applying $dm_i = \frac{\partial m_i}{\partial T} dT + \sum_j \frac{\partial m_i}{\partial n_j} dn_j$, then comparing the corresponding expression with Eq. (A2) we immediately have

$$\mu_i = \frac{\partial F_i}{\partial \mu_i^*} \frac{\partial \mu_i^*}{\partial n_i} + \sum_j \left(\frac{\partial F_j}{\partial m_j} + \frac{\partial F_j}{\partial \mu_j^*} \frac{\partial \mu_j^*}{\partial m_j} \right) \frac{\partial m_j}{\partial n_i}. \tag{A7}$$

and

$$S = -\sum_i \left[\frac{\partial F_i}{\partial T} + \frac{\partial F_i}{\partial \mu_i^*} \frac{\partial \mu_i^*}{\partial T} + \left(\frac{\partial F_i}{\partial m_i} + \frac{\partial F_i}{\partial \mu_i^*} \frac{\partial \mu_i^*}{\partial m_i} \right) \frac{\partial m_i}{\partial T} \right] \tag{A8}$$

To simplify the expressions, we differentiate Eqs. (A3) and (A5) to get

$$dn_i = \frac{\partial n_i}{\partial T} dT + \frac{\partial n_i}{\partial \mu_i^*} d\mu_i^* + \frac{\partial n_i}{\partial m_i} dm_i, \tag{A9}$$

$$d\mu_i^* = \frac{\partial \mu_i^*}{\partial T} dT + \frac{\partial \mu_i^*}{\partial n_i} dn_i + \frac{\partial \mu_i^*}{\partial m_i} dm_i, \tag{A10}$$

which implies

$$\frac{\partial \mu_i^*}{\partial T} \frac{\partial n_i}{\partial \mu_i^*} = -\frac{\partial n_i}{\partial T}, \quad \frac{\partial \mu_i^*}{\partial n_i} \frac{\partial n_i}{\partial \mu_i^*} = -1,$$
$$\frac{\partial \mu_i^*}{\partial m_i} \frac{\partial n_i}{\partial \mu_i^*} = -\frac{\partial n_i}{\partial m_i}. \tag{A11}$$

Defining

$$\Omega_0 \equiv \sum_i \Omega_{0,i}(T, \mu_i^*, m_i) = \sum_i [\Omega_{0,i}^+ + \Omega_{0,i}^-] \tag{A12}$$

with

$$\Omega_{0,i}^{\pm} = -\frac{g_i T}{2\pi^2} \int_0^{\infty} \ln[1 + e^{-(\sqrt{p^2 + m_i^2} \mp \mu_i^*)/T}] p^2 dp, \tag{A13}$$

then we can write $F_i = \Omega_{0,i} + \mu_i^* n_i$. Substituting this into Eq. (A8) and (A7), then applying Eq. (A11) and $n_i = -\partial \Omega_{0,i}/\partial \mu_i^*$, we have

$$\mu_i = \mu_i^* + \sum_j \frac{\partial \Omega_0}{\partial m_j} \frac{\partial m_j}{\partial n_i}. \tag{A14}$$

and

$$S = -\frac{\partial \Omega_0}{\partial T} - \sum_i \frac{\partial \Omega_0}{\partial m_i} \frac{\partial m_i}{\partial T}. \tag{A15}$$

Obviously, the free energy density can be given as

$$F = \Omega_0 - \sum_i \mu_i^* \frac{\partial \Omega_0}{\partial \mu_i^*}. \tag{A16}$$

The energy density is obtained by $E = F + TS$, giving

$$E = \Omega_0 - \sum_i \mu_i^* \frac{\partial \Omega_0}{\partial \mu_i^*} - T\frac{\partial \Omega_0}{\partial T} - T\sum_i \frac{\partial \Omega_0}{\partial m_i} \frac{\partial m_i}{\partial T}. \tag{A17}$$

And the pressure is obtained by substituting Eq. (A14) into Eq. (A1):

$$P = -\Omega_0 + \sum_{i,j} n_i \frac{\partial \Omega_0}{\partial m_j} \frac{\partial m_j}{\partial n_i}. \tag{A18}$$

Equations (A15)–(A18) here are in complete accordance with the Eqs. (58)–(61) in Ref. [19] if one regards the μ_i there as μ_i^* and Ω as Ω_0, which were not explicitly stated. The expression in Eq. (A14) is special in the present article because we need the real chemical potential to investigate the mixed phase.

The real thermodynamic potential density of the system is

$$\Omega = F - \sum_i \mu_i n_i = \Omega_0 - \sum_{i,j} n_i \frac{\partial \Omega}{\partial m_j} \frac{\partial m_j}{\partial n_i}. \quad (A19)$$

In the above derivation, we choose volume V, the temperature T, and the particle number densities n_i as the independent system variables. In this case, the free energy is the characteristic function from which we get the complete set of thermodynamic functions. For this purpose we have defined the intermediate variables μ_i^* in Eqs. (A4) and (30). Because the quark matter we are considering is a strongly interacting system, the relations between the chemical potentials and the densities are, in principle, not the same as those of a free Fermi gas. However, with the "effective" chemical potentials μ_i^*, the densities and the free energy are really of the same form as those of a noninteracting Fermi gas. This is what the "effective" means. The actual chemical potentials of each type of particles are determined from the fundamental thermodynamic equality (A2) that results in Eq. (A14).

[1] H. A. Bethe and G. E. Brown, Astrophys. J. **445**, L129 (1995).
[2] P. Haensel, M. Bejger, and J. L. Zdunik, arXiv: 0705.4594v1 [astro-ph].
[3] I. Bombaci, G. Lugones, and I. Vidana, Astron. Astrophys. **462**, 1017 (2007).
[4] M. G. Alford, K. Rajagopal, and F. Wilczek, Nucl. Phys. **B537**, 443 (1999).
[5] M. Huang and I. A. Shovkovy, Phys. Rev. D **70**, 051501 (2004); M. Huang and I. A. Shovkovy, Phys. Rev. D **70**, 094030 (2004).
[6] R. Casalbuoni, R. Gatto, M. Mannarelli, G. Nardulli, and M. Ruggieri, Phys. Lett. **B605**, 362 (2005); Phys. Lett. **B615**, 297 (2005).
[7] M. Alford and Qinghai Wang, J. Phys. G **31**, 719 (2005).
[8] K. Fukushima, Phys. Rev. D **72**, 074002 (2005).
[9] T. D. Li, Nucl. Phys. **A750**, 1 (2005).
[10] E. Witten, Phys. Rev. D **30**, 272 (1984).
[11] E. Farhi and R. L. Jaffe, Phys. Rev. D **30**, 2379 (1984); M. S. Berger and R. L. Jaffe, Phys. Rev. C **35**, 213 (1987); E. P. Gilson and R. L. Jaffe, Phys. Rev. Lett. **71**, 332 (1993).
[12] For a recent review, see R. M. Weiner, Int. J. Mod. Phys. E **15**, 37 (2006); and quoted therein.
[13] M. Buballa and M. Oertel, Phys. Lett. **B457**, 261 (1999).
[14] K. Schertler, C. Greiner, and M. H. Thoma, Nucl. Phys. **A616**, 659 (1997).
[15] A. B. Santra and U. Lombardo, Phys. Rev. C **62**, 018202 (2000).
[16] G. X. Peng, Nucl. Phys. **A747**, 75 (2005); G. X. Peng, M. Loewe, U. Lombardo, and X. J. Wen, Nucl. Phys. B Proc. Suppl. **133**, 259 (2004); G. X. Peng, H. C. Chiang, P. Z. Ning, U. Lombardo, and M. Loewe, Int. J. Mod. Phys. A **18**, 3151 (2003); G. X. Peng, U. Lombardo, M. Loewe, and H. C. Chiang, Phys. Lett. **B548**, 189 (2002).
[17] G. X. Peng, H. C. Chiang, J. J. Yang, L. Li, and B. Liu, Phys. Rev. C **61**, 015201 (1999).
[18] G. X. Peng, H. C. Chiang, B. S. Zou, P. Z. Ning, and S. J. Luo, Phys. Rev. C **62**, 025801 (2000).
[19] X. J. Wen, X. H. Zhong, G. X. Peng, P. N. Shen, and P. Z. Ning, Phys. Rev. C **72**, 015204 (2005).
[20] P. Grangé, A. Lejeune, M. Martzolff, and J.-F. Mathiot, Phys. Rev. C **40**, 1040 (1989).
[21] W. Zuo, A. Lejeune, U. Lombardo, and J.-F. Mathiot, Nucl. Phys. **A706**, 418 (2002); Eur. Phys. J. A **14**, 469 (2002).
[22] H. Q. Song, M. Baldo, G. Giansiracusa, and U. Lombardo, Phys. Rev. Lett. **81**, 1584 (1998).

[23] K. Schertler, S. Leupold, and J. Schaffner-Bielich, Phys. Rev. C **60**, 025801 (1999).
[24] M. Baldo, G. F. Burgio, P. Castorina, S. Plumari, and D. Zappala', Phys. Rev. C **75**, 035804 (2007); and references quoted therein.
[25] J. Madsen and J. M. Larsen, Phys. Rev. Lett. **90**, 121102 (2003).
[26] G. N. Fowler, S. Raha, and R. M. Weiner, Z. Phys. C **9**, 271 (1981).
[27] S. Chakrabarty, S. Raha, and B. Sinha, Phys. Lett. **B229**, 112 (1989); S. Chakrabarty, Phys. Rev. D **43**, 627 (1991); **48**, 1409 (1993); **54**, 1306 (1996).
[28] O. G. Benvenuto and G. Lugones, Phys. Rev. D **51**, 1989 (1995); G. Lugones and O. G. Benvenuto, Phys. Rev. D **52**, 1276 (1995); O. G. Benvenuto and G. Lugones, Int. J. Mod. Phys. D **7**, 29 (1998).
[29] G. X. Peng, H. C. Chiang, P. Z. Ning, and B. S. Zou, Phys. Rev. C **59**, 3452 (1999).
[30] Y. Zhang and R. K. Su, Phys. Rev. C **65**, 035202 (2002); Y. Zhang, R. K. Su, S. Q. Ying, and P. Wang, Europhys. Lett. **56**, 361 (2001); Y. Zhang and R. K. Su, Phys. Rev. C **67**, 015202 (2003).
[31] P. Wang, Phys. Rev. C **62**, 015204 (2000).
[32] G. X. Peng, P. Z. Ning, and H. Q. Chiang, Phys. Rev. C **56**, 491 (1997).
[33] X. P. Zheng, X. W. Liu, M. Kang, and S. H. Yang, Phys. Rev. C **70**, 015803 (2004).
[34] G. Lugones and J. E. Horvath, Int. J. Mod. Phys. D **12**, 495 (2003).
[35] X. J. Wen, G. X. Peng, and Y. D. Chen, J. Phys. G: Nucl. Part. Phys. **34**, 1697 (2007).
[36] X. J. WEN, G. X. PENG, and P. N. SHEN, Int. J. Mod. Phys. A **22**, 1649 (2007); G. X. Peng, X. J. Wen, and Y. D. Chen, Phys. Lett. **B633**, 313 (2006).
[37] A. Peshier, B. Kämpfer, and G. Soff, Phys. Rev. C **61**, 045203 (2000).
[38] W.-M. Yao *et al.*, J. Phys. G: Nucl. Part. Phys. **33**, 1 (2006).
[39] Z. H. Li, U. Lombardo, H.-J. Schulze, and W. Zuo, Phys. Rev. C **77**, 034316 (2008).
[40] A. Lejeune, P. Grangé. M. Martzolff, and J. Cugnon, Nucl. Phys. **A453**, 189 (1986).
[41] M. Baldo, I. Bombaci, L. S. Ferreira, G. Giansiracusa, and U. Lombardo, Phys. Lett. **B215**, 1 (1988).
[42] W. Zuo, Z. H. Li, A. Li, and G. C. Lu, Phys. Rev. C **69**, 064001 (2004).
[43] R. B. Wiringa, V. G. J. Stoks, and R. Schiavilla, Phys. Rev. C **51**, 38 (1995).

[44] R. Machleidt, Adv. Nucl. Phys. **19**, 189 (1989); R. Brockmann and R. Machleidt, Phys. Rev. C **42**, 1965 (1990); R. Machleidt, Phys. Rev. C **63**, 024001 (2001).

[45] M. Baldo and L. S. Ferreira, Phys. Rev. C **59**, 682 (1999).

[46] N. K. Glendenning, *Compact Stars* (Springer-Verlag, New York, 1996).

[47] N. K. Glendenning, Phys. Rev. D **46**, 1274 (1992).

[48] C. Maieron, M. Baldo, G. F. Burgio, and H.-J. Schulze, Phys. Rev. D **70**, 043010 (2004); O. E. Nicotra, M. Baldo, G. F. Burgio and H.-J. Schulze, *ibid*. **74**, 123001 (2006).

[49] W. Zuo, A. Li, Z. H. Li, and U. Lombardo, Phys. Rev. C **70**, 055802 (2004).

[50] G. E. Brown, C.-H. Lee, and M. Rho, Phys. Rept. **462**, 1 (2008).

[51] G. Q. Li, C. H. Lee, and G. E. Brown, Phys. Rev. Lett. **79**, 5214 (1997); F. Weber, Prog. Part. Nucl. Phys. **54**, 193–288 (2005); and quoted therein.

[52] G. F. Burgio, M. Baldo, P. K. Sahu, A. B. Santra, and H.-J. Schulze, Phys. Lett. **B562**, 19 (2002); G. F. Burgio, M. Baldo, P. K. Sahu, and H.-J. Schulze, Phys. Rev. C **66**, 025802 (2002).

[53] A. Li, G. F. Burgio, U. Lombardo, and W. Zuo, Phys. Rev. C **74**, 055801 (2006).